

Article

Temperature-Controlled Retinal Photocoagulation Reliably Generates Uniform Subvisible, Mild, or Moderate Lesions

Stefan Koinzer¹, Alexander Baade², Kerstin Schlott², Carola Hesse¹, Amke Caliebe³, Johann Roider¹, and Ralf Brinkmann²

¹ Department of Ophthalmology, University hospital of Schleswig-Holstein, Kiel, Germany

² Medical Laser Centre Lübeck GmbH, Lübeck, Germany

³ Institute of Medical Informatics and Statistics, University hospital of Schleswig-Holstein, Kiel, Germany

Correspondence: Stefan Koinzer, Department of Ophthalmology, University hospital of Schleswig-Holstein, Campus Kiel, House 25, Arnold-Heller-Str. 3, 24105 Kiel, Germany. e-mail: koinzer@auge.uni-kiel.de

Received: 10 April 2014

Accepted: 21 July 2015

Published: 6 October 2015

Keywords: spectral domain; OCT; laser photocoagulation; optoacoustics; real-time temperature measurement; animal model; subvisible

Citation: Koinzer S, Baade A, Schlott K, et al. Temperature-controlled retinal photocoagulation reliably generates uniform subvisible, mild, or moderate lesions. 2015;4(5):9, doi: 10.1167/tvst.4.5.9

Purpose: Conventional retinal photocoagulation produces irregular lesions and does not allow reliable control of ophthalmoscopically invisible lesions. We applied automatically controlled retinal photocoagulation, which allows to apply uniform lesions without titration, and aimed at five different predictable lesion intensities in a study on rabbit eyes.

Methods: A conventional 532-nm photocoagulation laser was used in combination with a pulsed probe laser. They facilitated real-time fundus temperature measurements and automatic exposure time control for different predefined time/temperature dependent characteristics (TTC). We applied 225 control lesions (exposure time 200 ms) and 794 TTC lesions (5 intensities, exposure times 7–800 ms) in six rabbit eyes with variable laser power (20–66.4 mW). Starting after 2 hours, we examined fundus color and optical coherence tomographic (OCT) images over 3 months and classified lesion morphologies according to a seven-stage OCT classifier.

Results: Visibility rates in funduscopy (OCT) after 2 hours were 17% (68%) for TTC intensity group 1, 38% (90%) for TTC group 2 and greater than 94% (>98%) for all consecutive groups. TTC groups 1 through 4 correlated to increasing morphological lesion intensities and increasing median funduscopy and OCT diameters. Group 5 lesions were as large as, but more intense than group 4 lesions.

Conclusions: Automatic, temperature controlled photocoagulation allows to apply predictable subvisible, mild, or moderate lesions without manual power titration.

Translational Relevance: The technique will facilitate standardized, automatically controlled low and early treatment of diabetic retinopathy study (ETDRS) intensity photocoagulation independently of the treating physician, the treated eye and lesion location.

Introduction

Retinal laser photocoagulation can preserve or even improve vision in spite of its tissue-destructive nature.^{1,2} Even today, in the era of vascular endothelial growth factor blocking intravitreal injections, laser photocoagulation remains the standard treatment of peripheral ischemic retinal conditions, such as severe diabetic retinopathy, retinal vein occlusion and others, and a second-line or adjunctive treatment of diabetic macular edema.³

Much effort has been undertaken recently to minimize side effects like pain, scotoma formation,

and others through softer lesions.⁴ One approach uses selective retina therapy (SRT), which aims at thermo-mechanical selective disruption of retinal pigment epithelial (RPE) cells. SRT induces a wound healing reaction in the RPE, thus improves metabolism at the chorioretinal junction and “rejuvenates” the RPE.^{5–7} Various other innovations like micropulse lasers⁸ or short exposure continuous wave (CW) lasers⁹ are capable to induce arbitrary mild damage in the retinal tissue or merely stimulate it thermally at a cell-preserving intensity level. Pilot studies have collected evidence that subvisible treatment and SRT are clinically effective.^{8,10–13} The term subvisible is

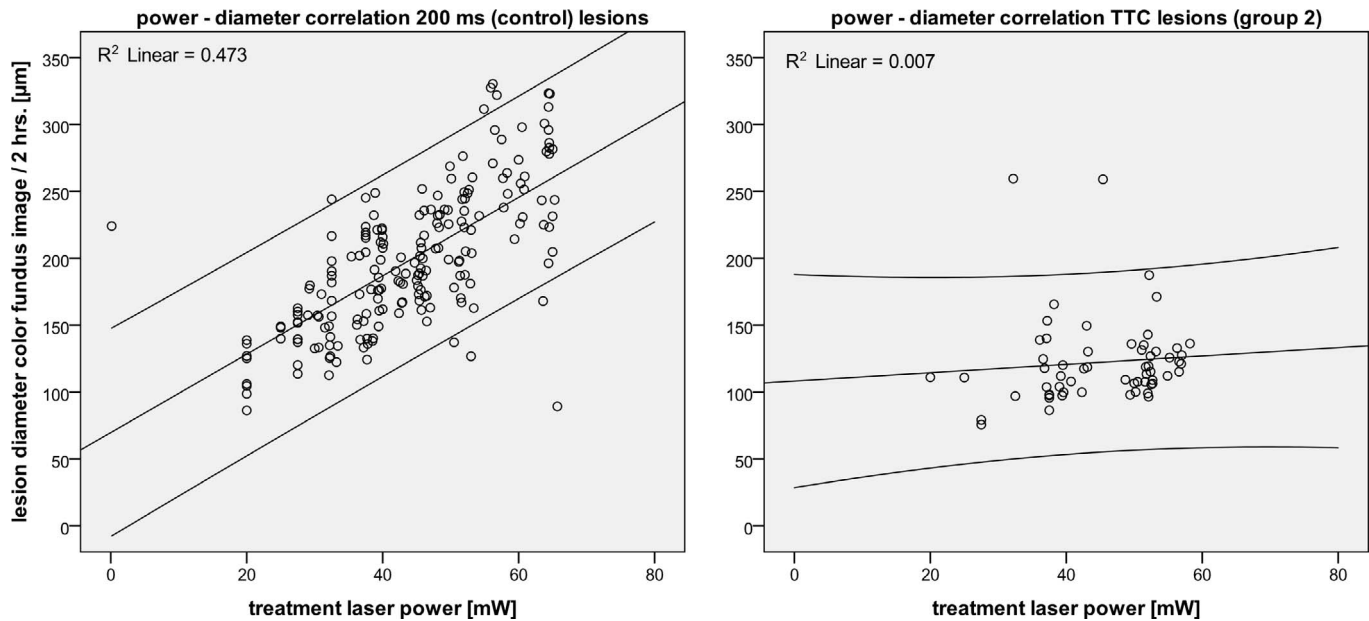


Figure 1. The linear correlations of treatment laser power with ophthalmoscopic diameter review the advantage of automatically controlled TTC photocoagulation.^{18,19} In standard, 200 ms lesions, the lesion diameters grows linearly with power ($R^2 = 0.5$, left), while this correlation is lost in TTC lesions ($R^2 = 0.0$, right, here for TTC subgroup two lesions of the present study). As TTC lesions are independent of power, they will not require power titration in a clinical setting and be uniform throughout patients and fundus locations, largely irrespective of local pigmentation and transmission. The *black lines* show the linear regressions (*middle*) and 95% CI's for prediction.

commonly applied for lesions that are at least ophthalmoscopically invisible during the treatment. Due to inter- and intraindividual variation of light transmission, light absorption, and tissue sensitivity, the biological effect of a laser irradiation cannot be predicted from laser parameters alone, such as power, irradiation time, and irradiation diameter. Effective control of the biological tissue effect has remained a key challenge in modern photocoagulation.^{9,14}

We have recently introduced fundus temperature measurement during photocoagulation.^{15–17} Based on temperature measurements, we implemented automatic exposure time control that produces homogeneous lesions widely independently of laser power or local absorption, respectively.^{18,19} The treatment device measures fundus temperature increments non-invasively in real-time with 1-kHz sampling rate and stops the treatment laser, when a predefined time-temperature characteristic (TTC) criterion is achieved. While in standard lesions with fixed exposure time, the ophthalmoscopic lesion diameter grows linearly with laser power, automatically TTC controlled lesions lose the correlation of power and lesion diameter (Fig. 1). They do not require titration and will be uniform throughout fundus locations, irrespective of fundus pigmentation, and patients. The

resulting lesions of the previous study were barely visible with a diameter equal to the irradiation beam.¹⁹

In the current study, we investigated modifications of the TTC criterion, in order to reliably generate photocoagulation lesions of different clinically desired, predictable intensities. Five different TTC intensities were evaluated in order to define adequate TTC criteria for subvisible and early treatment of diabetic retinopathy study (ETDRS)^{20,21} intensity treatments.

Materials and Methods

Animal Photocoagulation Study

We applied 1022 lesions in six eyes of three chinchilla gray rabbits. The animals were treated under general and local anesthesia, with dilated pupils. A modified Mainster focal grid laser contact lens was fitted onto the eye with methylcellulose gel (2%) and mechanically fixed in its position. We performed photocoagulation with a 532-nm continuous wave (CW) laser system (VISULAS 532s; Carl Zeiss Meditec AG, Jena, Germany).

The irradiation diameter was 133 μm on the rabbit

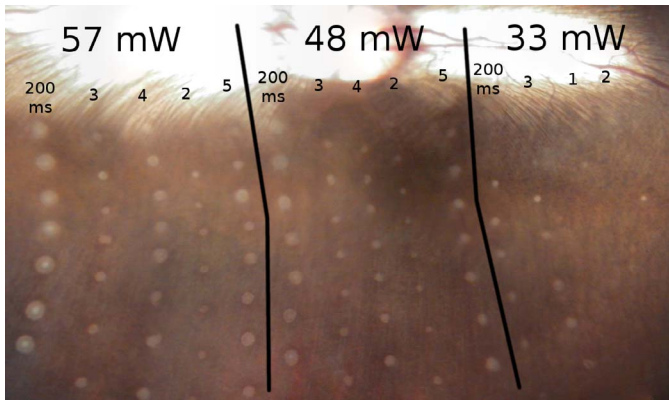


Figure 2. One representative rabbit fundus panorama, which was digitally assembled from several photographs taken 2 hours after laser treatment. Five columns on the left were applied with 55 mW, the following five columns were applied with 48 mW, and the four columns on the right were applied with 33 mW. Exposure times were 200 ms in the 1st, 6th, and 11th columns, and automatically controlled for different TTC intensities (1–5) in the rest. Thirty-three milliwatt power was not sufficient to achieve group 4 or 5 lesions within the maximum exposure time, while 48 and 55 mW powers were too high to achieve group 1 lesions even in the shortest possible exposure time. Therefore, not all TTC groups were applied with every power setting.

fundus. Exposure times were 200 ms or variable, automatically controlled for five different TTC intensities. For 200 ms standard irradiations, we adjusted laser power in order to achieve ophthalmoscopically visible lesions of various intensities, but no ruptures or bleedings. Next to a column of 200 ms lesions, we applied columns of different intensity TTC lesions using the same power setting. TTC exposure time control is limited to a certain ideal exposure time window¹⁹ that we defined to be 10 to 800 ms in the present study. Only those TTC groups were applied that were likely to achieve the intended intensity within 10 to 800 ms. Figure 2 shows a fundus image after one of the experiments. The figure has been digitally assembled from several single images using Hugin software version 2010.2.0 (www.hugin.sourceforge.net).

The rabbits were maintained in animal units at the University Medical Centre of Schleswig-Holstein, and all animal experiments were performed according to the German law for protection of animals and approved by the Ministry of Energy Transition, Agriculture, Environment and Rural Areas of Schleswig-Holstein, Kiel, Germany (application no. V312-7234.121-11). All experiments adhered to the ARVO Statement for the Use of Animals in Ophthalmic and Vision Research.

Fundus Temperature Measurement

We measured the fundus temperature profile during treatment laser irradiation in real-time and noninvasively on the basis of optoacoustics as published before.^{15–17,22} In short, we superimposed a pulsed 523-nm laser (75 ns pulses, 3–8 μ J; QG-523-1000; Crysta-Laser LC, Reno, NY), collinearly and coaxially to the treatment irradiation. The pulses were emitted at a repetition rate of 1 kHz and caused short, innocuous temperature increments within the irradiated tissue that induced short, reversible thermoelastic tissue expansions. The amplitude of these expansions depends on the tissue temperature. Tissue expansions cause ultrasonic pressure waves that propagate through the eye, and these were detected by an embedded transducer in the custom made, modified contact lens (Mod. Mainster OMRA-S, Ocular Instruments, Bellevue, WA, modified by Medical Laser Centre Lübeck GmbH). Its signals were digitally processed and recorded via a digital/analog transducer card in a personal computer. The signal profile reflects relative changes of the average tissue temperature within the probed tissue volume. “Tissue volume” refers to all tissue layers that are traversed by the light beam with a given diameter and that absorb irradiation, such as RPE, pigmented choroid, and to a lesser extent retina, choriocapillaris, and others. By solving the heat diffusion equation, we calculated peak temperature in the lesion center at the RPE level.

Automatic Exposure Time Control

Based on fundus temperature monitoring and processing in real time, the irradiation could be stopped as soon as the desired TTC criterion was met. Figure 3 shows schematically the strategy of the automatic switch-off algorithm for three differently pigmented fundus locations, in order to achieve uniform lesions.

The shutoff mechanism for subvisible or barely visible lesions is based on a characteristic curve that correlates the induced temperature over time with a certain lesion size. The characteristic curve for a 95% probability to create visible lesions of the desired size (expected dose 95/ED95) was determined previously.^{18,19} The characteristic curve was fitted using the damage integral from the Arrhenius theory, which describes the relationship between thermal denaturation of proteins over time and the temperature course,^{18,23} by stepwise time integration over the expected denaturation or damage, respectively. The

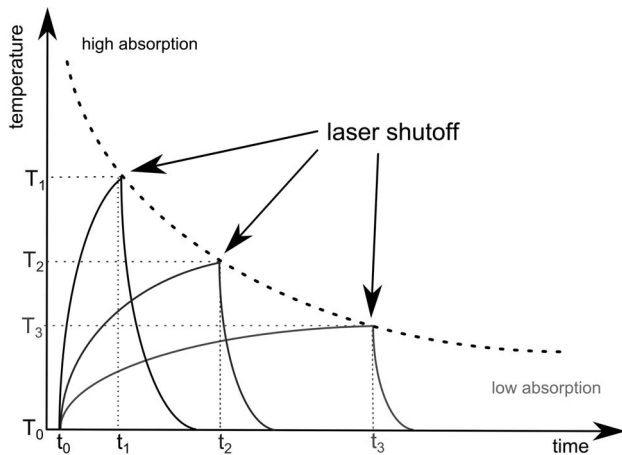


Figure 3. Schematic diagram of an arbitrary TTC curve. The Arrhenius theory supplies a mathematical model of the time-dependent tissue effect of a temperature increase, and served as a source for our empirically adapted TTC curves. All time-temperature combinations that meet one particular TTC curve will induce equal lesions. Short exposures require higher temperatures than long exposures in order to achieve an equal effect (if $T_1 > T_2$, then $t_1 < t_2$). Vertical transposition of the TTC plot allows modifying lesion intensities.

fit enabled us to calculate the ED95 temperature thresholds for arbitrary exposure times.

For stronger, suprathreshold lesions, accurate temperature measurement is impossible with this device. The tissue begins to coagulate during treatment, which compromises the initial pressure-to-temperature calibration. In order to estimate tissue coagulation, we formulated a particular damage function that evaluated both calibrated and uncalibrated optoacoustic transients. After empirical adjustments, this formula provided the characteristic curves used in this study.

Five different characteristic curves for different uniform lesion strengths were found. Besides a previously published TTC criterion¹⁹ (which corresponds to the TTC group 3 in this study), two lower intensities (groups 1, 2) and two higher intensities (groups 4, 5) were introduced in the present study.

Color Fundus Imaging and Retinal Lesion Diameter Assessment

We obtained fundus color photographs 2 hours after the treatment, using a Zeiss VISUCAM (Carl Zeiss Meditec AG). Three observers measured the lesion areas in these images. Edematous halos were excluded from the measurements, because they represent surrounding subretinal edema, but not retinal denaturation.^{24–26} Every lesion was outlined

manually in image editing software (GIMP Ver. 2.8., www.gimp.org), its pixel size measured in ImageJ software (www.rsweb.nih.gov/ij/) and the pixel and real circle diameters calculated. The pixel-to-micrometer scale was $9.5 \pm 0.7 \mu\text{m}/\text{pixel}$.²⁷ If only one observer recognized a particular lesion, it was classified invisible (diameter 0), otherwise the mean diameter was used as an estimate of the real spot size. Comparing the three measurements, we excluded out-of-range values as defined previously.²⁴ We chose that method in order to rule out any observer-dependency and bias in the assessment of faint and/or poorly outlined fundus lesions.

OCT Analysis

OCT images were acquired after 2 hours, 1 week, 1 and 3 months. We scanned the treated area in 30- μm steps using a spectral-domain OCT (HRA + OCT Spectralis; Heidelberg Engineering, Heidelberg, Germany). We averaged 20 B-scans per sectional image and traced every lesion through consecutive OCT series using the AutoRescan function.

The greatest linear diameter (GLD) of a lesion was measured in the proprietary software of the OCT machine. We measured the GLD at the photoreceptor inner segment-to-outer segment junction line or, if this measurement was not unequivocal, at the RPE level. Each sectional image that showed a lesion was thoroughly reviewed, and the widest diameter passing through the lesion was measured as GLD.

In order to assess the burn intensity of each lesion, we graded lesions on 2 hour OCT images according to a seven-stage classifier that we had validated and published separately.²⁴ Characteristics of these intensity classes are reviewed in Figure 4. Lesion intensity will be referred to by the term “OCT class.”

Statistics

We used Fisher’s exact test for the analysis of the association of two categorical variables, such as TTC group and OCT class, or visibility. We calculated corresponding *P* values on the basis of Monte-Carlo simulations ($n = 10,000$ samples). The influence of a categorical variable, like TTC group, on a continuous variable, like diameter, was tested nonparametrically in a Kruskal-Wallis test. These tests were performed for the entire sample and for each of the six rabbit eyes separately. The tests were adjusted for multiple testing by the Bonferroni-method. The correlation of laser power and ophthalmoscopic lesion diameter was evaluated by simple linear

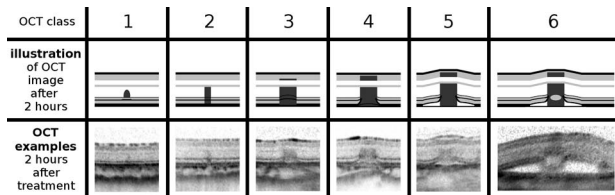


Figure 4. Summary of OCT-based lesion intensity classes that were used in this study. The *upper row* shows a schematic drawing of characteristic OCT changes for each class. The *lower row* shows an OCT example taken 2 hours after exposure. Seven lesion classes were defined as follows: Class 0: Lesion never became detectable in OCT images (not shown). Class 1: Thickening of the inner segment (IS) – outer segment (OS) junction line, and slight darkening of the outer nuclear layer (ONL). These lesions may be easily missed in OCT images. Class 2: *Dark column* throughout the OS, IS and ONL layers, wider than in a class 1 lesion. The external limiting membrane (ELM) remains flat. Class 3: Thinning of the RPE. Upward protrusion of IS–OS junction line and ELM, but preserved layer continuity. Darkening includes partial thickness of the inner plexiform layer (IPL) but is discontinuous and spares the outer plexiform layer (OPL). Class 4: RPE is detached from Bruch’s membrane (BM) and protrudes upward, while the space in between remains dark. *Dark OS tips*, IS–OS junction line and ELM are interrupted and bent upward at the lesion border. OS tips and IS–OS junction lines merge at the lesion border. IPL darkening increases compared to class 3. Class 5: Perilesional neurosensory detachment, which protrudes the entire retina upward. Facultative discoloration of the ganglion layer (GL). Class 6: *Additional bright spot* in the *dark central column* at the level of the PS. Facultative full thickness darkening including OPL and inner nuclear layer (INL); Figure and description modified from Koinzer et al. 2013.²⁴ Courtesy of Wiley-Blackwell publishers).

regression. All tests performed were two sided. P values below 0.05 were considered statistically significant. All statistical analyses were carried out with SPSS software, version 20 (IBM Corp., Armonk, NY).

Results

We applied 1022 photocoagulation lesions in six eyes of three rabbits. The irradiation diameter on the fundus was 133 μm . Power was varied from 20 to 66.4 mW, and exposure times that the automatic algorithm adjusted ranged from 7 to 1384 ms. In three lesions, automatic TTC control failed, and exposures were continued beyond the preselected maximum interval of 800 ms, up to 1384 ms. Failure was due to calibration errors or false parameter settings. These three lesions were excluded from the analysis. Four lesions were exposed less than 10 ms, but at least 7 ms, and were included in the analysis.

Of 1022 lesions, 225 were control lesions (200 ms,

power range 20–65.7 mW, and power variation 329%). Automatically controlled lesions were applied in five TTC groups, where TTC group 1 indicates the softest lesions and TTC group 5 the most intense lesions. One hundred nineteen lesions were TTC group 1 (20–50.1 mW, 251%), 141 TTC group 2 (20–58.1 mW, 291%), 223 TTC group 3 (20–65.2 mW, 326%), 190 TTC group 4 (25–56.5 mW, 226%), and 124 TTC group 5 lesions (27.5–66.4 mW, 241%). The distribution of treatment laser powers in each TTC group is shown in histogram plots in [Supplementary Figure S1](#).

A complete dataset including a 2 hour fundus color image, and 2 hour, 1 week, 1 and 3 months OCT images as well could be obtained of 486 lesions, 22 of which were covered by but undetectable in OCT images. We conducted several analyses that did not require all of these data, such as presented in [Figure 5](#), where only 2 hour images were used, which allowed us to use a greater number of lesions for evaluation. Likewise, sample sizes differ in other analyses as well ([Fig. 5–7](#), [Table 1](#)) and are indicated in each Figure separately.

Qualitative Lesion Evaluation ([Fig. 2](#))

[Figure 2](#) shows a fundus image 2 hours after photocoagulation. The diameters of 200 ms exposure lesions vary significantly with power. TTC groups that were created with different power settings appear more homogenous than standard lesions. TTC group 2 lesions are close to the threshold of ophthalmoscopic visibility and may, or may not, be visible, while group 1 lesions are mostly invisible ([right](#)).

Correlation of Laser Power and Ophthalmoscopic Diameter

The diameter of ophthalmoscopically visible lesions correlates linearly to laser power for fixed exposure time ([Fig. 1](#), left).^{19,28} In our study, the linear R^2 value was 0.473 for standard 200 ms lesions. The corresponding R^2 values for TTC groups 1 through 5 were less than 0.001, 0.007 ([Fig. 1](#), right), 0.049, 0.066, and 0.051. Thus, TTC lesions show no (linear) correlation of fundus diameter and laser power. This confirms statistically the qualitative findings from [Figure 2](#).

Threshold Evaluation ([Fig. 5](#))

[Figure 5](#) shows the percentages of lesions that were visible in fundus color images (red) and OCT images (gray) after 2 hours in each TTC group. The influence of the TTC group was significant for both (Fisher’s exact

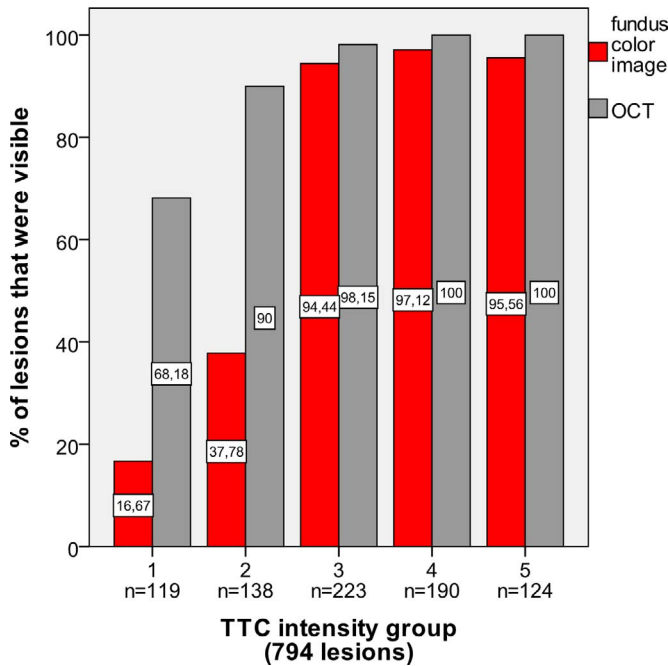


Figure 5. Percentages of lesions in each TTC group that became detectable in fundus color images (red bars) and OCT images (gray bars) after 2 hours. The impact of the TTC group on both parameters was significant ($P < 0.001$). Sample sizes for TTC groups are indicated at the x-axis. Seven hundred ninety-four lesions qualified for evaluation.

test, $P < 0.001$). In TTC group 1, only 17% of lesions became visible on the fundus image after 2 hours, but 68% could be detected in OCT images. In TTC group 2, 38% of lesions were detected on fundus images, but 90% in OCT. As visibility on the fundus increases over time after lesion application, and immediate ophthalmoscopic judgement is less sensitive than triple evaluation of highly upscaled digital images as performed in this study, TTC groups 1 and 2 were invisible during the treatment and would qualify clinically as subvisible lesions. OCT proves that the majority of TTC group 1 and 2 lesions had a biomorphological effect. For higher TTC groups 3 to 5, visibility was greater than 94% in both imaging modalities.

With regard to threshold evaluations, one has to keep in mind the proper definition of a threshold. Calculation of threshold powers or temperatures in photocoagulation is usually done by probit analyses, where the threshold indicates power or temperature values with a 50% chance to achieve a visible lesion (ED50). As the biological effect of identical stimuli varies, even if the temperature is controlled, we cannot expect to determine TTC groups that are completely invisible on the fundus, or completely detectable in OCT.

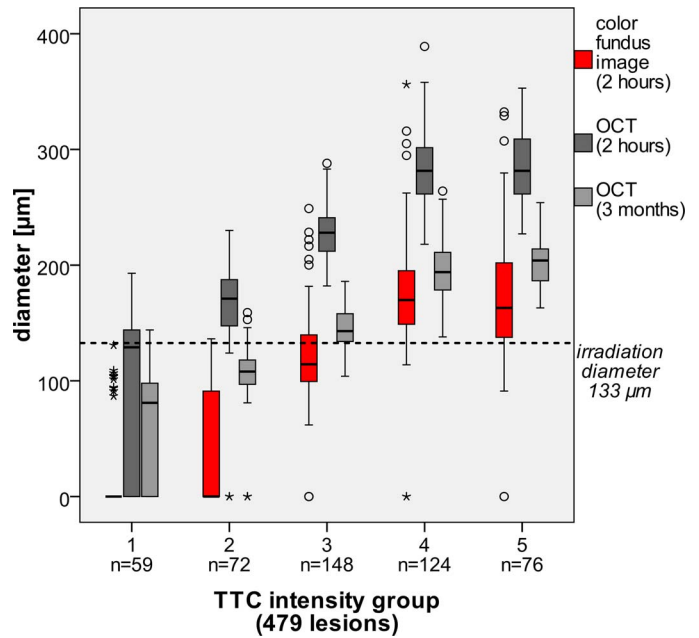


Figure 6. Box plots of the parameters ophthalmoscopic diameter after 2 hours (red), OCT GLD after 2 hours (dark gray) and OCT GLD after 3 months (light gray) for each TTC group. A dotted horizontal line indicates the irradiated diameter of 133 µm. The same data and P values are given numerically in Table 1. Sample sizes for TTC groups are indicated at the x-axis. Four hundred seventy-nine lesions qualified for evaluation.

Lesion Diameters (Fig. 6, Table 1)

Figure 6 and Table 1 show box plots and numerical data of lesion diameters in fundus images after 2 hours and in OCT images after 2 hours and 3 months. All three parameters correlate significantly with the TTC group, which applies to the global analysis and to separate analyses of each of the six rabbit eyes as well (each of 21 Kruskal-Wallis tests: $P \leq 0.001$). Automatic laser exposure control worked properly in each rabbit eye. Imaging data acquired after 1 and 4 weeks are consistent with and redundant to these findings and are therefore not shown.

Ophthalmoscopic lesion diameters were smaller than GLD values after 2 hours, but GLD's shrunk over 3 months. All three parameters, ophthalmoscopic diameter, OCT GLD after 2 hours and OCT GLD after 3 months, increased significantly with TTC groups 1 to 4, but remained constant between groups 4 and 5, as is confirmed by pairwise comparison (Table 1). TTC group 3 produces lesions equally large in fundus color images as the irradiation beam. OCT GLD's of these group 3 lesions have not been measured before.¹⁹ Groups 4 and 5 have equal diameters that are larger than the corresponding values for group 3.

Table 1. Lesion Diameters of Different TTC Groups, Shown Numerically for Ophthalmoscopic Diameters after 2 Hours and OCT GLD's after 2 Hours and 3 Months

TTC Group	n	Ophthalmoscope Diameter		GLD		GLD	
		2 h, μm	P Value [Pairwise]	2 h, μm	P Value [Pairwise]	3 mo, μm	P Value [Pairwise]
1	59	0 (0–0)		129 (0–144)		81 (0–98)	
2	72	0 (0–93)	1 vs. 2 < 0.001	171 (147–188)	1 vs. 2 < 0.001	108 (97–118)	1 vs. 2 < 0.001
3	148	114 (99–140)	2 vs. 3 < 0.001	228 (212–241)	2 vs. 3 < 0.001	143 (134–158)	2 vs. 3 < 0.001
4	124	170 (149–195)	3 vs. 4 < 0.001	282 (261–302)	3 vs. 4 < 0.001	194 (178–211)	3 vs. 4 < 0.001
5	76	163 (137–202)	4 vs. 5 1	282 (260–309)	4 vs. 5 1	204 (186–214)	4 vs. 5 1
P			< 0.001		< 0.001		< 0.001

The same data are displayed graphically in [Figure 6](#). The table shows median and interquartile range (IQR) values. Below each column, *P* values for the indicated parameter are given, and in each line, *P* values of pairwise comparisons (Kruskal-Wallis test). Only lesions with a complete data set (2 hour color fundus images and two consecutive OCT images) were included in the evaluation. All values increase for TTC groups 1 through 4 and remain stable between groups 4 and 5.

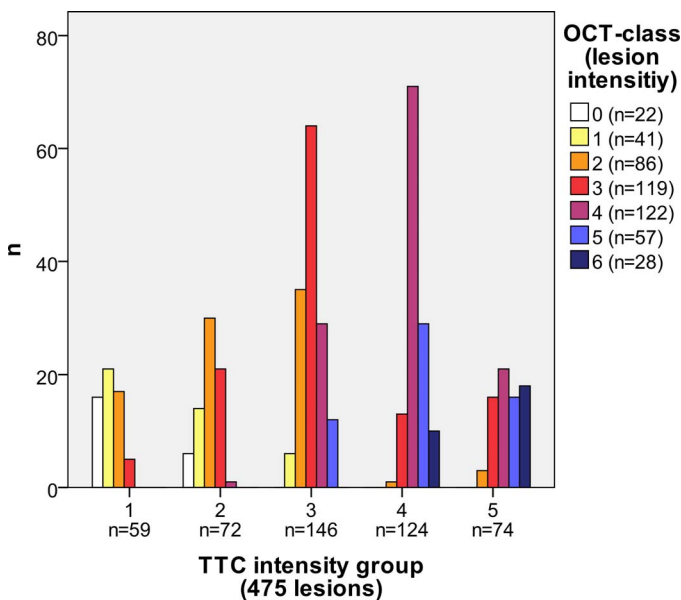


Figure 7. The distribution of OCT lesion classes for all TTC groups in absolute numbers. OCT classes reflect lesion intensity, or axial extension, respectively. The classes are displayed by *different color bars* as indicated in the legend, with increasing intensity from *white via red to blue*. Sample sizes are given for OCT classes in the legend and for TTC groups at the x-axis. Four hundred seventy-five lesions qualified for evaluation. Lesion intensity increases significantly with the TTC group ($P < 0.001$).

Lesion Intensities ([Fig. 7](#))

Control lesions achieved OCT classes 2 to 6, but never class 1 (data not shown, for class definitions see [Fig. 4](#)).

[Figure 7](#) shows how OCT classes were distributed in each TTC group. OCT classes reflect the intensity of a lesion, or the axial extent, respectively.²⁴ The correlation of TTC groups and OCT classes was statistically significant (Fisher's exact test, $P < 0.001$). TTC group 1 achieved predominantly class 1 lesions, but also a significant proportion of class 0 lesions, which were invisible in OCT images (see also [Fig. 5](#)). TTC group 2 achieved predominantly class 2 lesions and only very few class 0 lesions. The predominating OCT classes were 3 in TTC group 3, and 4 in TTC group 4. In TTC group 5, classes 3 to 6 occurred almost equally, but classes 5 and 6 occurred more often than in TTC group 4. TTC group 5 showed the most severe photocoagulation damage, but more lesion variability than other TTC groups.

Discussion

In this study, we evaluated a novel photocoagulation exposure time control, which is intended to automatically create reproducible photocoagulation

lesions independently of lesion location, individual eye and treating physician. The treatment device measures fundus temperature increments noninvasively in real-time with 1-kHz sampling rate¹⁶ and stops the treatment laser, when a predefined TTC criterion is achieved.¹⁸ Five different TTC intensities were evaluated clinically in order to define adequate TTC criteria for subvisible and ETDRS intensity treatments.

We applied 1022 photocoagulation lesions. Lesion visibility after 2 hours allowed identifying of subvisible lesions, and lesion diameters and GLD's after 2 hours and 3 months allowed to evaluate lesion homogeneity. In order to assess lesion intensity, or axial extension, respectively, we applied a recently published OCT-based grading system²⁴ that differentiates one undetectable and six detectable lesion classes in 2 hour OCT images. We consider this to be the most important measure, as axial lesion extension correlates with functional damage to the retinal nerve fibre layer, which is thought to cause extended scotoma and should therefore be avoided.

Conventional judgement of photocoagulation lesions evaluates retinal whitening in three or four categories,^{29–31} which is observer-dependent and requires evaluation by several investigators in clinical trials.³² The judgement depends on the latency from application to evaluation as well.²⁵ The lack of prospective lesion control carries the risk of significant misdoseage if fundus susceptibility to laser irradiation varies strongly from one lesion to the next. These disadvantages have already been realized more than 30 years ago.³³ but none of the earlier approaches solved the problem.^{34–36}

The therapeutic window of retinal photocoagulation is defined to be the ratio of laser power that induces retinal rupture by the power that induces retinal blanching. The therapeutic window is wide enough for treatment according to ETDRS requirements (>50 ms).³⁷ It narrows for shorter exposure times and closes at approximately 1 ms, where retinal whitening and rupture occur at similar power settings.³⁸ Nonetheless, lesion complications like choroidal bleeding remain an exception even in 20-ms exposures.^{39,40} We have previously shown that the temperature range of ETDRS 20 to 200 ms lesions is large. These lesions are created in patients at peak temperatures of approximately 95°C up to 180°C,¹⁷ the latter being the calculated threshold for retinal rupture.³⁸ For this reason, panretinal ETDRS lesions can be safely created with conventional laser power control in spite of its shortcomings, but they do show significant variability.¹⁷

Optoacoustics enable accurate temperature measurements only in native tissue conditions. In cases of significant tissue coagulation during treatment irradiation, the thermomechanical characteristics of the tissue will change. Consequently, temperature monitoring becomes less accurate, and the uniformity of the resulting automatically controlled lesions is impaired in high TTC groups. This study was partly designed to find the upper intensity limit that TTC control can safely produce, and it seems to be TTC group 5. Group 5 lesions were stronger, but less homogenous than TTC group 4 lesions. TTC group 5 lesions have gentle necrotic cores (Fig. 2) and correspond to the intensity commonly applied in panretinal ETDRS lesions, which are sought to induce “moderate” whitening. Hence, the introduced exposure time control would allow to create intensities up to ETDRS panretinal lesions, but most likely not for retinopexy at this stage. Improved temperature-based shutoff strategies may solve this problem, such as predictive exposure time calculation based on temperature data measured during the initial milliseconds of a treatment. Failure of TTC in 3 of 797 lesions had other reasons and did not occur in group 5 lesions.

TTC dosage addresses primarily softer lesions. The temperature range of subvisible lesions is less than 10°C, as the RPE viability threshold has been found to be about 53°C,^{38,41} and visible lesions in rabbits and patients are created at temperatures of little above 60°C (OCT class 2 and 3 at 200 ms).^{17,24} The temperature increments from one OCT class to the next in 200 ms lesions are in the order of 5°C for OCT classes 3 to 5 and about 10°C for classes 5 to 6 (in rabbits). The corresponding temperatures for 100 ms lesions have never been determined, but patient data imply that these values should be very similar (difference to 200 ms thresholds is estimated at 1°C to 2°C).¹⁷ It is obvious that standard laser dosage on the basis of ophthalmoscopic visibility must fail in these small temperature ranges, particularly for lesions that are not even visible on the fundus. Even in TTC lesions, there is some variability, which becomes obvious through the width of whiskers in Figure 6 and through the range of OCT classes achieved for each TTC intensity class (Fig. 7).

There are essentially three sources of lesion variability in this study. The first is variability of the biological response to identical thermal stimuli, which is inevitable. The second is inaccuracy of experimental lesion assessment. We used an elaborate diameter assessment protocol and established an OCT classifier to retrieve information on axial lesion extension, but

even these optimized methods do not have perfect objectivity and reliability. The third source of variability is inaccuracy of the laser dosage device. Our setup does not allow to determine the particular impact of either of the three contributing factors. Nevertheless, each TTC group limited the range of OCT classes sufficiently to allow reliable creation of sub- or suprathreshold lesions or to avoid damage to the retinal nerve fibre layer.

Certain technical limits of optoacoustic temperature determination, which postulates homogenous tissue pigmentation in its computational model and becomes invalid once tissue coagulation sets in, could be overcome by OCT-based temperature determination as we have shown in a previous publication.⁴² OCT-based automated photocoagulation dosage is, however, not yet available due to its technical complexity.

In our study, the TTC algorithm compensated for natural pigmentation variations of 200% to 300% on the fundus³⁸ and was still capable to level power variations of 226% to 326% within the desired exposure time frame, giving a good therapeutic window. Even outside this window, like in lesions with inadequately high power setting or unexpectedly high light transmission to a densely pigmented area of retina, severe overtreatment can be reliably prevented by exposure time reduction down to 4 ms.¹⁹ On the other hand, undertreatment would occur in lesions that fail to meet the TTC criterion within 800 ms. In a clinical setting, the software could inform the surgeon about under- or overtreatment if exposure times exceed the 10- to 800-ms range, and remind him to adjust power properly. Alternatively, a self-learning algorithm could adjust treatment power automatically. This would represent a significant progress compared with the clinical state-of-the-art.

Over the past 10 years, various studies have applied lesions softer than ETDRS intensity clinically, and many of those pilot-type studies showed promising results.^{8,10–13,43,44} In those studies, lesion intensities were controlled by a variety of inconsistent criteria, which produced different outcomes, makes lesion characteristics incompatible and prevents meta-analyses. Automatic laser exposure control as presented in this study is, to the authors' knowledge, the only functional way to accurately create well-defined lesion intensities above and below the visibility threshold. Possible intensities include subvisible lesions, which we defined to be visible in OCT but invisible on the fundus during the treatment (TTC groups 1–2), very soft lesions as would be appropriate for (modified) ETDRS macular treatment (TTC groups 3–4) or for ETDRS

panretinal treatment (TTC groups 4–5). Thermally stimulating lesions that remain undetectable even in OCT could most likely be created as well by appropriate adaptation of the TTC curve.

Conclusions

The presented technique facilitates automatic standardized fundus lesions that are independent of treating physician, individual eye, and treatment location. The method would, for the first time, allow objective dosage of laser photocoagulation lesions. This is a prerequisite for controlled clinical trials that investigate the minimal clinically effective lesion intensity of retinal photocoagulation. The transfer of optoacoustic real-time fundus temperature detection to patients has already been successful,¹⁷ and automatic exposure control shall be at hand for clinical pilot studies shortly. In a patient application, the accuracy of lesion reproducibility should be clinically confirmed, and TTC criteria might need some adaptation from rabbit to human conditions, but those issues appear fairly easy to handle.

Acknowledgments

Supported by grants from the German Ministry of Education and Research (BMBF) according to the Innovation Award for Advancing Medical Technology 2006, grant #01EZ0734 (Department of Ophthalmology, University hospital of Schleswig-Holstein, Campus Kiel), #01EZ0732 (Medical Laser Centre Lübeck), #01EZ0733 (Institute of Biomedical Optics Lübeck), and #01EZ0735 (Carl Zeiss Meditec AG).

The research presented here has been subject of a poster presentation at the 2013 ARVO annual meeting (program no. 4131).

Disclosure: **S. Koinzer**, None; **A. Baade**, None; **K. Schlott**, None; **C. Hesse**, None; **A. Caliebe**, None; **J. Roeder**, None; **R. Brinkmann**, Patent rights

A German translation of the abstract is available in the supplemental material.

References

1. The Diabetic Retinopathy Study Research Group. Preliminary report on effects of photo-

- coagulation therapy. *Am J Ophthalmol.* 1976;81:383–396.
2. The Diabetic Retinopathy Study Research Group. Photocoagulation treatment of proliferative diabetic retinopathy: the second report of diabetic retinopathy study findings. *Ophthalmology* 1978;85:82–106.
 3. Shah AM, Bressler NM, Jampol LM. Does laser still have a role in the management of retinal vascular and neovascular diseases? *Am J Ophthalmol.* 2011;152:332–339.e1.
 4. Fong DS, Girach A, Boney A. Visual side effects of successful scatter laser photocoagulation surgery for proliferative diabetic retinopathy: a literature review. *Retina* 2007;27:816–824.
 5. Brinkmann R, Roider J, Birngruber R. Selective retina therapy (SRT): a review on methods, techniques, preclinical and first clinical results. *Bull Soc Belge Ophthalmol.* 2006;302:51–69.
 6. Roider J, Lindemann C, el-Hifnawi S, Laqua H, Birngruber R. Therapeutic range of repetitive nanosecond laser exposures in selective RPE photocoagulation. *Graefes Arch Clin Exp Ophthalmol.* 1998;236:213–219.
 7. Pelosini L, Hamilton R, Mohamed M, Hamilton AP, Marshall J. Retina rejuvenation therapy for diabetic macular edema: a pilot study. *Retina* 2013;33:548–558.
 8. Luttrull JK, Musch DC, Spink CA. Subthreshold diode micropulse panretinal photocoagulation for proliferative diabetic retinopathy. *Eye* 2008;22:607–612.
 9. Lavinsky D, Sramek C, Wang J, et al. Subvisible retinal laser therapy: titration algorithm and tissue response. *Retina* 2014;34:87–97.
 10. Koinzer S, Elsner H, Klatt C, et al. Selective retina therapy (SRT) of chronic subfoveal fluid after surgery of rhegmatogenous retinal detachment: three case reports. *Graefes Arch Clin Exp Ophthalmol.* 2008;246:1373–1378.
 11. Roider J, Liew SHM, Klatt C, et al. Selective retina therapy (SRT) for clinically significant diabetic macular edema. *Graefes Arch Clin Exp Ophthalmol.* 2010;248:1263–1272.
 12. Klatt C, Saeger M, Oppermann T, et al. Selective retina therapy for acute central serous chorioretinopathy. *Br J Ophthalmol.* 2011;95:83–88.
 13. Lavinsky D, Cardillo JA, Melo LAS Jr, Dare A, Farah ME, Belfort R Jr. Randomized clinical trial evaluating mETDRS versus normal or high-density micropulse photocoagulation for diabetic macular edema. *Invest Ophthalmol Vis Sci.* 2011;52:4314–4323.
 14. Luttrull JK, Sramek C, Palanker D, Spink CJ, Musch DC. Long-term safety, high-resolution imaging, and tissue temperature modeling of subvisible diode micropulse photocoagulation for retinovascular macular edema. *Retina* 2012;32:375–386.
 15. Kandulla J, Elsner H, Birngruber R, Brinkmann R. Noninvasive optoacoustic online retinal temperature determination during continuous-wave laser irradiation. *J Biomed Opt.* 2006;11:041111.
 16. Brinkmann R, Koinzer S, Schlott K, et al. Real-time temperature determination during retinal photocoagulation on patients. *J Biomed Opt.* 2012;17:061219.
 17. Koinzer S, Schlott K, Portz L, et al. Correlation of temperature rise and optical coherence tomography characteristics in patient retinal photocoagulation. *J Biophotonics* 2012;5:889–902.
 18. Schlott K, Koinzer S, Ptaszynski L, et al. Automatic temperature controlled retinal photocoagulation. *J Biomed Opt.* 2012;17:061223.
 19. Koinzer S, Schlott K, Ptaszynski L, et al. Temperature controlled retinal photocoagulation—a step toward automated laser treatment. *Invest Ophthalmol Vis Sci.* 2012;53:3605–3614.
 20. Early Treatment Diabetic Retinopathy Study research group. Photocoagulation for diabetic macular edema. Early Treatment Diabetic Retinopathy Study report number 1. *Arch Ophthalmol.* 1985;103:1796–1806.
 21. Early Treatment Diabetic Retinopathy Study Research Group. Early photocoagulation for diabetic retinopathy. ETDRS report number 9. *Ophthalmology.* 1991;98:766–785.
 22. Baade A, Schlott K, Luft S, et al. Accuracy of real-time optoacoustic temperature determination during retinal photocoagulation. *Proc SPIE.* 2011;8092:80921B.
 23. Birngruber R, Hillenkamp F, Gabel VP. Theoretical investigations of laser thermal retinal injury. *Health Phys.* 1985;48:781–796.
 24. Koinzer S, Hesse C, Caliebe A, et al. Photocoagulation in rabbits: optical coherence tomographic lesion classification, wound healing reaction, and retinal temperatures. *Lasers Surg Med.* 2013;45:427–436.
 25. Weinberg W, Gabel V-P, Birngruber R, Lorenz B, Müller W. Time Sequence of the White Hue Correlated with the Extent of Damage in Photocoagulation of the Retina [article in German]. *Ber Dtsch Ophthalmol Ges.* 1981;78:603–606.
 26. Koinzer S, Saeger M, Hesse C, et al. Correlation with OCT and histology of photocoagulation

- lesions in patients and rabbits. *Acta Ophthalmol.* 2013;91:e603–e611.
27. Koinzer S, Bajorat S, Hesse C, et al. Calibration of histological retina specimens after fixation in Margo's solution and paraffin embedding to in-vivo dimensions, using photography and optical coherence tomography. *Graefes Arch Clin Exp Ophthalmol.* 2014;252:145–153.
 28. Jain A, Blumenkranz MS, Paulus Y, et al. Effect of pulse duration on size and character of the lesion in retinal photocoagulation. *Arch Ophthalmol.* 2008;126:78–85.
 29. Tso MO, Wallow IH, Elgin S. Experimental photocoagulation of the human retina. I. Correlation of physical, clinical, and pathologic data. *Arch Ophthalmol.* 1977;95:1035–1040.
 30. Muqit MMK, Marcellino GR, Henson DB, Fenerty CH, Stanga PE. Randomized clinical trial to evaluate the effects of pascal panretinal photocoagulation on macular nerve fibre layer: Manchester Pascal Study Report 3. *Retina.* 2011;31:1699–1707.
 31. Palanker D, Lavinsky D, Blumenkranz MS, Marcellino G. The impact of pulse duration and burn grade on size of retinal photocoagulation lesion: implications for pattern density. *Retina* 2011;31:1664–1669.
 32. Kang H, Su L, Zhang H, Li X, Zhang L, Tian F. Early histological alteration of the retina following photocoagulation treatment in diabetic retinopathy as measured by spectral domain optical coherence tomography. *Graefes Arch Clin Exp Ophthalmol.* 2010;248:1705–1711.
 33. Birngruber R, Gabel VP, Hillenkamp F. Fundus reflectometry: a step towards optimization of the retina photocoagulation. *Mod Probl Ophthalmol.* 1977;18:383–390.
 34. Inderfurth J, Ferguson R, Frish M, Birngruber R. Dynamic Reflectometer for Control of Laser Photocoagulation on the Retina. *Lasers Surg Med.* 1994;15:54–61.
 35. Jerath MR, Chundru R, Barrett SF, Rylander HG III, Welch AJ. Reflectance feedback control of photocoagulation in vivo. *Arch Ophthalmol.* 1993;111:531–534.
 36. Pomerantzeff O, Wang GJ, Pankratov M, Schneider J. A method to predetermine the correct photocoagulation dosage. *Arch Ophthalmol.* 1983;101:949–953.
 37. Mainster MA. Decreasing retinal photocoagulation damage: principles and techniques. *Semin Ophthalmol.* 1999;14:200–209.
 38. Sramek C, Paulus Y, Nomoto H, Huie P, Brown J, Palanker D. Dynamics of retinal photocoagulation and rupture. *J Biomed Opt.* 2009;14:034007.
 39. Velez-Montoya R, Guerrero-Naranjo JL, Gonzalez-Mijares CC, et al. Pattern scan laser photocoagulation: safety and complications, experience after 1301 consecutive cases. *Br J Ophthalmol.* 2010;94:720–724.
 40. Muqit MMK, Marcellino GR, Henson DB, et al. Single-session vs multiple-session pattern scanning laser panretinal photocoagulation in proliferative diabetic retinopathy: the Manchester Pascal Study. *Arch Ophthalmol.* 2010;128:525–533.
 41. Denton ML, Noojin GD, Foltz MS, et al. Spatially correlated microthermography maps threshold temperature in laser-induced damage. *J Biomed Opt.* 2011;16:036003.
 42. Mueller HH, Ptaszynski L, Schlott K, et al. Imaging thermal expansion and retinal tissue changes during photocoagulation by high speed OCT. *Biomed Opt Express* 2012;3:1025–46.
 43. Figueira J, Khan J, Nunes S, et al. Prospective randomised controlled trial comparing sub-threshold micropulse diode laser photocoagulation and conventional green laser for clinically significant diabetic macular oedema. *Br J Ophthalmol.* 2009;93:1341–1344.
 44. Bandello F, Brancato R, Menchini U, et al. Light panretinal photocoagulation (LPRP) versus classic panretinal photocoagulation (CPRP) in proliferative diabetic retinopathy. *Semin Ophthalmol.* 2001;16:12–18.